

# An eigenvalue method using multiple frequency data for inverse scattering problems

Jiguang Sun\*

## Abstract

Dirichlet and transmission eigenvalues have important applications in qualitative methods in inverse scattering. Motivated by the fact that these eigenvalues can be obtained from scattering data, we propose a new eigenvalue method using multiple frequency data (EM<sup>2</sup>F). The method detects eigenvalues and builds indicator functions to reconstruct the support of the target. Numerical reconstruction is quite satisfactory. In addition, estimation of Dirichlet or transmission eigenvalues can be obtained. Furthermore, reconstruction of  $D$  and estimation of eigenvalues can be combined together to distinguish between the sound soft obstacle and non-absorbing inhomogeneous medium.

## 1 Introduction

Dirichlet and transmission eigenvalues play important roles in qualitative methods in inverse scattering [1]. The Dirichlet eigenvalue problem has been well-studied. Transmission eigenvalue problem is fairly new and its research developed quickly recently [24, 14, 22, 20, 6]. Based on theoretical investigation, new qualitative methods have emerged to estimate index of refraction using transmission eigenvalues [4, 3, 25]. Numerical methods to compute transmission eigenvalues and the corresponding interior transmission problem are developed as well [13, 26, 17].

It is known that transmission eigenvalues can be estimated from far field data by the linear sampling method (LSM) [2]. It is also possible to do this using near field Cauchy data [25]. In fact, Dirichlet eigenvalues or transmission eigenvalues can be estimated from either far field or near field data [2, 5].

There are only a few works on qualitative methods using multiple frequency data. In [21], Luke and Potthast established conditions on the time-dependent waves that provide a correspondence between time domain and frequency domain inverse scattering via Fourier transforms. Then they applied the result to extend the point source method to scattering from the pulses. Chen et al. proposed a time domain linear sampling method [7]. In [16], Guzina et al. investigated the possibility of multi-frequency reconstruction of sound soft and penetrable obstacles via the linear sampling method. It is also worth to mention the work by Colton and Monk [12] which uses Herglotz wave functions at first Dirichlet eigenvalue to find the shape of scatterers.

---

<sup>1</sup>Department of Mathematical Sciences, Delaware State University, Dover, DE 19901, U.S.A.  
E-mail: jsun@desu.edu

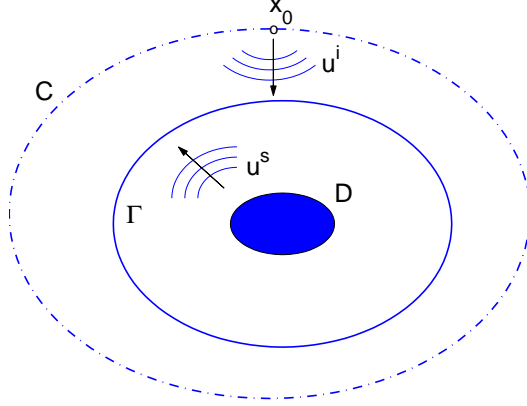


Figure 1: Explicative Example. We assume that the target  $D$  is inside some domain  $\Omega$  ( $\Gamma := \partial\Omega$ ) which itself is inside a curve  $C$ . The scattered field  $u^s$  is due to the scattering of the incident field  $u^i$  due to a point source at  $x_0 \in C$

In this paper, we propose an eigenvalue method using multiple frequency data (EM<sup>2</sup>F). The EM<sup>2</sup>F detects Dirichlet or transmission eigenvalues of the target and builds indicator functions to reconstruct the support of the target. Estimation of eigenvalues can also be obtained. Furthermore, the method can distinguish between the sound soft obstacle and non-absorbing inhomogeneous medium.

We consider two cases: 1) the sound soft obstacle, and 2) the inhomogeneous medium. We assume that the target  $D$  is inside some domain  $\Omega$  which itself is inside a curve  $C$  (see Fig. 1). Let  $k$  be the wave number. The scattered field  $u^s$ , which will be specified later for sound soft obstacles and inhomogeneous media, respectively, is due to the scattering of the incident field  $u^i$  due to a point source at  $x_0 \in C$  given by

$$(1.1) \quad u^i(x, x_0) := \Phi(x, x_0), \quad x_0 \in C$$

where  $\Phi(x, x_0)$  is the fundamental solution of the Helmholtz equation in  $\mathbb{R}^2$ . We assume that  $u^s$  is measured on  $\Gamma = \partial\Omega$  for all point sources  $x$ 's on  $C$ .

In the following, we will need the near field operator  $\mathcal{N} : L^2(\Gamma) \rightarrow L^2(C)$  such that for  $v \in L^2(\Gamma)$ ,

$$(1.2) \quad (\mathcal{N}v)(x) = \int_{\Gamma} u^s(y, x)v(y)ds(y), \quad x \in C.$$

The near field linear sampling method is based on solving linear ill-posed integral equations

$$(1.3) \quad (\mathcal{N}v)(x) = \Phi(x, z) \quad \text{for all } x \in C$$

where  $z \in T$ , a sampling domain inside  $\Omega$  containing the target. It is well-known that the above equation does not have a solution in general. However, it

is possible to find an approximate solution of (1.3) and use the linear sampling method to reconstruct  $D$  except a discrete set of wave number  $k$ 's. These wave numbers are Dirichlet eigenvalues for sound soft obstacles or transmission eigenvalues for inhomogeneous media. In fact, this is the case we are interested in, i.e., detecting Dirichlet eigenvalues or transmission eigenvalues from the near field data  $u^s$  on  $\Gamma$  and use them to reconstruct  $D$ .

To solve (1.3) we need to use a convenient family of functions for  $v$ . In particular, we use the Herglotz wave functions defined as

$$v = \mathcal{H}g := \int_{\Omega} e^{ikx \cdot d} g(d) ds_d, \quad g \in L^2(S^1),$$

where  $S^1 = \{x \in \mathbb{R}^2, |x| = 1\}$ .

The rest of the paper is organized as follows. In Section 2, we introduce two scattering problems and illustrate how Dirichlet or transmission eigenvalues can be determined from the scattering data using the LSM. In Section 3, we propose an eigenvalue method using multiple frequency data. Numerical examples show that the method can provide excellent reconstruction for  $D$ . We will also explain how to obtain Dirichlet or transmission eigenvalues and distinguish sound soft obstacle and inhomogeneous medium from each other. Finally, in Section 4, we draw conclusions and discuss some future work.

## 2 The determination of eigenvalues

### 2.1 Scattering by a sound soft obstacle

We first consider the scattering problem for the sound soft obstacle. We assume that  $D \subset \mathbb{R}^2$  is an open, bounded region with Lipschitz boundary  $\partial D$ . The direct problem is to find a solution  $u \in H_{loc}^1(\mathbb{R}^2 \setminus \{x_0\})$  such that

$$(2.4a) \quad \Delta u + k^2 u = 0 \quad \text{in } \mathbb{R}^2 \setminus \{x_0\},$$

$$(2.4b) \quad u = u^i + u^s,$$

$$(2.4c) \quad u = 0 \quad \text{on } \partial D,$$

$$(2.4d) \quad \lim_{r \rightarrow \infty} \sqrt{r} \left( \frac{\partial u^s}{\partial r} - iku^s \right) = 0,$$

where  $u^i$  is the incident field due to a point source  $x_0$  on  $C$ . The following theorem is of fundamental importance for the LSM to reconstruct  $D$  (see [10]).

**Theorem 2.1.** *Assume that  $k^2$  is not a Dirichlet eigenvalue for  $D$ . Let  $\mathcal{N}$  be the near-field operator defined by (1.2).*

(a) *If  $z \in D$  then there exist a sequence  $\{v_n\}$  such that*

$$\lim_{n \rightarrow \infty} \mathcal{N}v_n = \Phi(\cdot, z).$$

*Furthermore,  $v_n$  converges in  $L^2(D)$ .*

(b) *If  $z \in \Omega \setminus D$  then for every sequence  $\{v_n\}$  such that*

$$\lim_{n \rightarrow \infty} \mathcal{N}v_n = \Phi(\cdot, z)$$

and we have that

$$\lim_{n \rightarrow \infty} \|v_n\|_{L^2(D)} = \infty.$$

Let  $\mathcal{N}^\delta$  be the near field operator corresponding to the noisy measurement. We assume that, for all points  $z \in D$ , the perturbed operator  $\mathcal{N}^\delta$  satisfies

$$(2.5) \quad \lim_{\delta \rightarrow 0} \|\mathcal{N}^\delta \mathcal{H}g_{z,\delta} - \Phi(\cdot, z)\|_{L^2(\Gamma)} = 0.$$

The Tikhonov regularized solution  $g_{z,\epsilon}^\delta$  of the near field equation is defined as the unique minimizer of the Tikhonov functional

$$(2.6) \quad \|\mathcal{N}^\delta(\mathcal{H}g) - \Phi(\cdot, z)\|_{L^2(\Gamma)}^2 + \epsilon \|g\|_{L^2(S^1)}^2$$

where  $\epsilon$  is the regularization parameter. We denote  $g_{z,\epsilon(\delta)}^\delta$  by  $g_{z,\delta}$  when  $\epsilon = \epsilon(\delta) \rightarrow 0$  as  $\delta \rightarrow 0$ .

In this paper, we are interested in the case when  $k$  is a Dirichlet eigenvalue. The following theorem addresses the behavior of  $\mathcal{H}g_{z,\delta}$ . Its proof is similar to Theorem 2.1 of [2] and thus we omit it here.

**Theorem 2.2.** *Let  $k^2$  be a Dirichlet eigenvalue and assume that (2.5) is true. Then for almost every  $z \in D$ ,  $\|\mathcal{H}g_{z,\delta}\|_{H^1(D)}$  cannot be bounded as  $\delta \rightarrow 0$ .*

Combining Theorems 2.1 and 2.2, if we choose a point  $z$  inside  $D$  and plot the norms of the kernels of the regularized solutions against the wave number  $k$ , we would expect the norms are relatively large when  $k$  is a Dirichlet eigenvalue and relatively small otherwise.

## 2.2 Scattering by an inhomogeneous medium

Next we consider the problem of scattering by an inhomogeneous medium. The direct problem is to find a solution  $u \in H_{loc}^1(\mathbb{R}^2 \setminus \{x_0\})$  such that

$$(2.7a) \quad \Delta u + k^2 n(x)u = 0 \quad \text{in } \mathbb{R}^2 \setminus \{x_0\},$$

$$(2.7b) \quad u = u^i + u^s,$$

$$(2.7c) \quad \lim_{r \rightarrow \infty} \sqrt{r} \left( \frac{\partial u^s}{\partial r} - iku^s \right) = 0,$$

where  $n(x)$  is the index of refraction and  $D := \text{supp}(n(x) - 1)$ . The corresponding transmission eigenvalue problem is to find  $k \in \mathbb{C}$ ,  $w, v \in L^2(D)$ ,  $w - v \in H^2(D)$  such that

$$(2.8a) \quad \Delta w + k^2 n(x)w = 0, \quad \text{in } D,$$

$$(2.8b) \quad \Delta v + k^2 v = 0, \quad \text{in } D,$$

$$(2.8c) \quad w - v = 0, \quad \text{on } \partial D,$$

$$(2.8d) \quad \frac{\partial w}{\partial \nu} - \frac{\partial v}{\partial \nu} = 0, \quad \text{on } \partial D,$$

where  $\nu$  is the unit outward normal to the boundary  $\partial D$  and the index of refraction  $n(x)$  is positive. Values of  $k \neq 0$  such that there exists a nontrivial

solution to (2.8) are called transmission eigenvalues. The existence of transmission eigenvalues has been studied by many researchers recently and we refer the readers to [24, 22, 20, 6] and the references therein.

The following theorem justifies the LSM for the scattering of inhomogeneous medium (see [10] for the case of far field data and [9] for using the reciprocity gap method).

**Theorem 2.3.** *Assume that  $k$  is not a transmission eigenvalue for  $D$ . Let  $\mathcal{N}$  be the near-field operator defined by (1.2).*

(a) *If  $z \in D$  then there exist a sequence  $\{v_n\}$ , such that*

$$\lim_{n \rightarrow \infty} \mathcal{N}v_n = \Phi(\cdot, z).$$

*Furthermore,  $v_n$  converges in  $L^2(D)$ .*

(b) *If  $z \in \Omega \setminus D$  then for every sequence  $\{v_n\}$ , such that*

$$\lim_{n \rightarrow \infty} \mathcal{N}v_n = \Phi(\cdot, z)$$

*we have that*

$$\lim_{n \rightarrow \infty} \|v_n\|_{L^2(D)} = \infty.$$

We consider the similar case of noisy data. It can be shown that if  $k$  is not a transmission eigenvalue then  $\mathcal{H}g_{z,\delta}$  converges in the  $H^1(D)$  norm as  $\delta \rightarrow 0$  for  $z \in D$ . For the case when  $k$  is a transmission eigenvalue, we assume that, for  $z \in D$ , the perturbed operator  $\mathcal{N}^\delta$  satisfies

$$(2.9) \quad \lim_{\delta \rightarrow 0} \|\mathcal{N}^\delta \mathcal{H}g_{z,\delta} - \Phi(\cdot, z)\|_{L^2(\Gamma)} = 0.$$

If the operator  $\mathcal{N}$  has dense range, the above assumption is true [2]. It is well-known that  $\mathcal{N}$  has dense range except when  $k$  is a transmission eigenvalue associated with non-trivial solutions  $(w_0, v_0)$  of (2.8) such that  $v_0$  can be represented as a Herglotz wave function [11].

The following theorem shows the behavior of the solution of (2.6) when  $k$  is a transmission eigenvalue. Its proof is similar to Theorem 3.2 in [2].

**Theorem 2.4.** *Let  $k$  be a transmission eigenvalue and assume that (2.9) is verified. Then for almost every  $z \in D$ ,  $\|\mathcal{H}g_{z,\delta}\|_{L^2(D)}$  cannot be bounded as  $\delta \rightarrow 0$ .*

Combining Theorems 2.4 and 2.3, if we choose a point  $z$  inside  $D$  and plot the norms of the kernels of the regularized solutions against the wave number  $k$ , we would expect the norms are relatively large when  $k$  is a transmission eigenvalue and relatively small otherwise.

## 2.3 Numerical results

We show numerically that Dirichlet eigenvalues and transmission eigenvalues can be detected from near field data by the LSM. The synthetic data is obtained using a finite element method. We solve the scattering problems on a mesh fine enough for wave numbers in an interval containing the lowest eigenvalue. We

Table 1: The exact Dirichlet eigenvalues.

$D$	1st	2nd	3rd	4th
circle	4.8172	7.6911	7.6923	10.3408
ellipse	5.1007	7.2977	8.8791	9.6219

Table 2: The exact transmission eigenvalues for  $n = 16$ .

$D$	1st	2nd	3rd	4th
circle	1.9907	2.6181	2.6183	3.2361
ellipse	2.1876	2.5565	3.0705	3.1088

put 40 point sources on the curve  $C$  which is the circle with radius 6. We record the scattered field  $u^s$  on the circle with radius 3 ( $\partial\Omega$ ) and add 3% noise. Then we choose a point inside  $D$  and solve the ill-posed integral equation (1.3) using Tikhonov regularization with Morozov discrepancy. Note that we assume that the support of  $D$  is known (approximately) as a priori which can be obtained by the LSM using the scattering data when  $k$  is not a eigenvalue. Finally we plot the norm of the Herglotz kernel  $g$  against the wave number  $k$ .

We choose two objects, a disk with  $r = 1/2$  and an ellipse whose axes are 0.6 and 0.4, in the test. For comparison, we first compute Dirichlet eigenvalues and transmission eigenvalues for  $n = 16$  for both objects and list them in Tables 1 and 2. We refer the readers to [13, 26] for numerical methods to compute transmission eigenvalues.

We first consider the case of scattering by a sound soft obstacle. We plot the norm of the Herglotz kernel v.s. the wave number in Fig. 2 for  $z = (-0.1, 0.1)$  inside the target. It can be seen that both pictures indicates the presence of Dirichlet eigenvalues. Comparing with the values in Tables 1 and 2, for both targets, the lowest a few Dirichlet eigenvalues can be determined from the near field data with satisfactory accuracy.

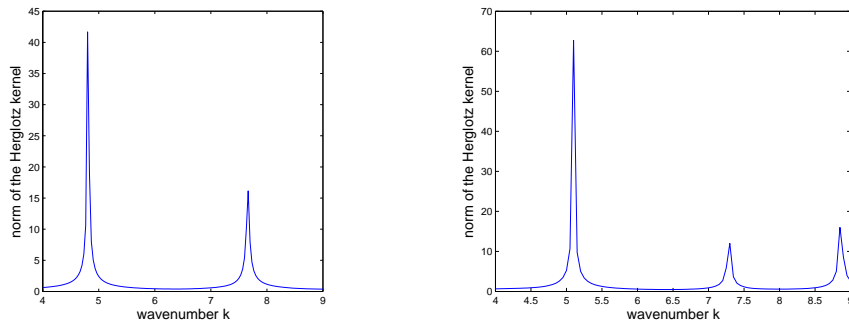


Figure 2: Estimation of Dirichlet eigenvalues. The plot of the norm of the Herglotz kernel v.s. the wave number for  $z = (-0.1, 0.1)$  inside the target. Left: The disk with  $r = 1/2$ . Right: The ellipse whose axis are 0.6 and 0.4.

Next we consider the case when the target is an inhomogeneous medium. For simplicity we set  $n = 16$ . The case when  $n(x)$  is a function is similar [25]. We plot the norm of the Herglotz kernel v.s. the wave number in Fig. 3 for  $z = (0.1, -0.2)$  inside the target. It can be seen that in both pictures the lowest transmission eigenvalues can be determined with good accuracy. We refer the readers to [5] for more numerical results and [25] for a similar computation using the reciprocity gap method.

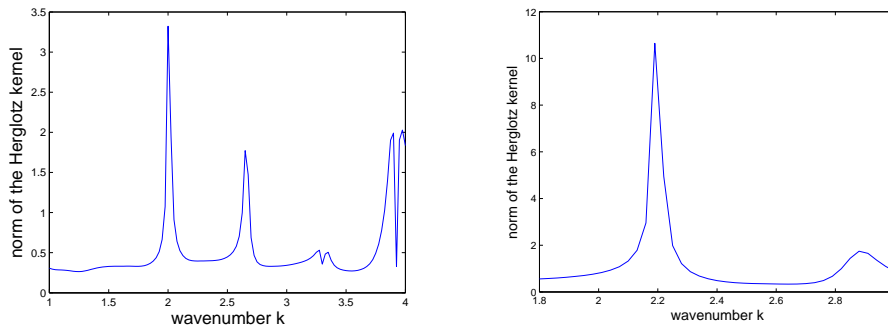


Figure 3: Estimation of transmission eigenvalues. The norm of the Herglotz kernel v.s. the wave number for  $z = (0.1, -0.2)$  inside the target. Left: The disk with  $r = 1/2$  when  $n = 16$ . Right: The ellipse whose axis are 0.6 and 0.4 when  $n = 16$ .

### 3 The EM<sup>2</sup>F

We have shown that the estimation of eigenvalues can be obtained provided a knowledge of a point  $z$  inside  $D$ . In this section, we assume no a priori information about the scattering object and illustrate how the EM<sup>2</sup>F works.

#### 3.1 The eigenvalue indicator

The idea of the EM<sup>2</sup>F to reconstruct the support of  $D$  relies on the detection of eigenvalues. Let  $\Lambda$  be the set of either transmission eigenvalues or Dirichlet eigenvalues. We first choose a sampling domain  $T$  containing  $D$ . For a point  $z$  in the sampling domain, if the behavior of the norm of the solutions is similar to those in Figures 2 and 3 indicating the existence of eigenvalues,  $z$  is deemed to be inside  $D$ . For this purpose, we first choose an interval for wave number  $F_k = [k_a, k_b]$  such that  $\Lambda \cap F_k \neq \emptyset$  and consider a partition  $F_k^i = \{k_i, i = 0, \dots, N\}$  of  $F_k$ . Note that  $\Lambda \cap F_k \neq \emptyset$  is not a restrictive requirement since one can choose  $k_a$  close to zero and a rather large  $k_b$ . Let  $u^s(y, x, k_i)$  be the scattered field of (2.4) or (2.7) and  $v(y, k_i)$  be the Herglotz wave function. We formulate the multiple frequency near field integral operator

$$(3.10) \quad (\mathcal{N}v)(x, k_i) = \int_{\Gamma} u^s(y, x, k_i)v(y, k_i)ds(y), \quad x \in C, \quad k_i \in F_k^i.$$

Similarly, we set up the near field integral equations

$$(3.11) \quad (\mathcal{N}v)(\cdot, k_i) = \Phi(\cdot, z, k_i), \quad k_i \in F_k^i.$$

As in the previous section, we seek the regularized solutions for each  $z$  in the sampling domain  $T$  and wave number  $k_i$  in  $F_k^i$ . Finally we define an eigenvalue indicator function

$$(3.12) \quad I_z = \frac{\max_i H_z(k_i)}{\sum_i H_z(k_i)/N}, \quad z \in T$$

where  $H_z(k_i)$  is the vector of norms of the Herglotz kernels of the regularized solutions for (3.11). Considering the results of the previous section (see Figures 2 and 3), we assume that a relatively large  $I_z$ , which might indicate the presence of eigenvalues, implies  $z$  is inside  $D$ .

Now we show some numerical examples. The forward problems are again solved using the finite element method and 3% noise is added to the computed scattered fields  $u^s$  for each wave number  $k_i \in F_k^i$ . Same targets as in the previous section are used for the tests. The sampling domain  $T$  is chosen to be  $[-1, 1] \times [-1, 1]$  containing  $D$ . We first consider the case of sound soft obstacles. For the disk with radius  $r = 1/2$ , we set  $F_k = [4.5, 5.0]$  and

$$F_k^i = \left\{ 4.5 + i \times \frac{5.0 - 4.5}{40}, i = 0, 1, 2, \dots, 40. \right\}.$$

For the ellipse, we set  $F_k = [5.0, 5.5]$  and

$$F_k^i = \left\{ 5.0 + i \times \frac{5.5 - 5.0}{40}, i = 0, 1, 2, \dots, 40. \right\}.$$

From Tables 1 and 2, we know both intervals contain Dirichlet eigenvalues for the circle and ellipse, respectively. Note that we could choose larger intervals which needs more computation time. We solve the near field equations for each  $k_i$  at the sampling point  $z$ . Then we compute the indicator functions defined in (3.12) for all sampling points.

In Fig. 4, we show the plots of the indicator function  $I_z$  for the two sound soft obstacles. We can clearly see the object which are a circle and an ellipse, respectively. The behavior of the approximate solution of (3.11) for  $z$  outside  $D$  is not clear at this point. Fortunately, the indicator function for  $z$  outside  $D$  is much smaller and the reconstruction is quite satisfactory. In fact, our numerical results indicate that  $H_z(k_i)$  is smaller for  $z \in \partial D$ .

Next we consider the case of inhomogeneous media. The index of refraction  $n$  is set to be 16. For the disk with radius  $r = 1/2$ , we set  $F_k = [1.8, 2.2]$  and

$$F_k^i = \left\{ 1.8 + i \times \frac{2.2 - 1.8}{20}, i = 0, 1, 2, \dots, 20. \right\}.$$

For the ellipse, we set  $F_k = [2.0, 2.4]$  and

$$F_k^i = \left\{ 2.0 + i \times \frac{2.4 - 2.0}{20}, i = 0, 1, 2, \dots, 20. \right\}.$$

Both intervals contain transmission eigenvalues for the circle and ellipse, respectively. Again we assume that the scattered fields are available for all the wave

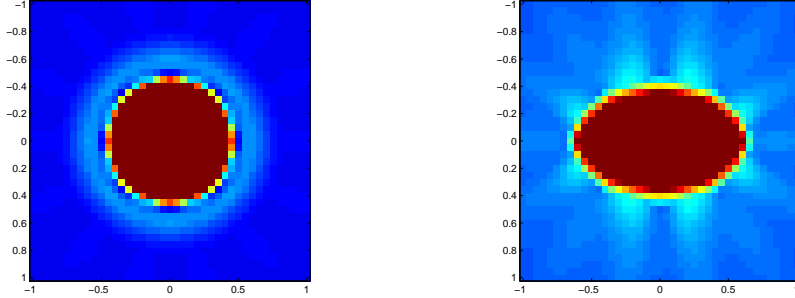


Figure 4: Reconstruction (plot of  $I_z$ ) of the sound soft obstacles using the eigenvalue indicator. Left: The target is a disk with  $r = 1/2$ . Right: The target is an ellipse whose axes are 0.6 and 0.4.

numbers in  $F_k^i$ 's and we solve the near field equations (3.11) for each  $k_i$  at the sampling point  $z$ . Then we compute the indicator functions defined in (3.12) for all sampling points in  $T$ .

In Fig. 5, we show the plots of the indicator function  $I_z$  for two non-absorbing inhomogeneous media. The objects can be seen clearly as well. Note that the reconstruction of inhomogeneous media by the linear sampling type methods are usually not as satisfactory as for sound soft obstacles [23].

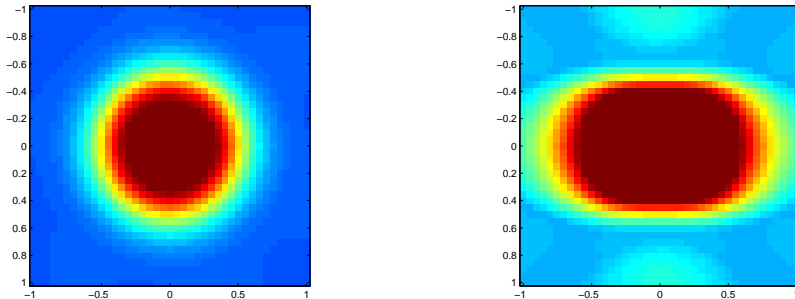


Figure 5: Reconstruction (plot of  $I_z$ ) of inhomogeneous media using the eigenvalue indicator. Left: The target is a disk with  $r = 1/2$ . Right: The target is an ellipse whose axes are 0.6 and 0.4.

### 3.2 The gradient indicator

Theorems 2.2 and 2.4 only consider the case of  $z \in D$ . It is desirable to know what happens when  $z \in \mathbb{R} \setminus D$ . Our numerical results show that the norm of regularized solution of (3.11) is relative small for  $z \in \partial D$  when  $k^2$  is an eigenvalue. In fact it can be verified that  $\|\mathcal{H}g_{z,\delta}\|_{L^2(D)}$  should be bounded as  $\delta \rightarrow 0$  for the simple case when  $\partial D$ ,  $\Gamma$  and  $C$  are all circles centered at the

origin. Moreover, the norm of the regularized solution is rather stable for  $z \in D$  and the change for  $z$  from inside  $D$  to  $\partial D$  is quite sharp (see Fig. 4 and Fig. 5).

Based on the above observation, the gradient of the eigenvalue indicator should change fast around the boundary of the target. Thus we define the gradient indicator as

$$(3.13) \quad G_z = \|\nabla I_z\|_{L^2}, \quad z \in T.$$

In the numerical implementation, since we have  $I_z$  on discrete points in the sampling domain  $T$ , we can compute the discrete gradient and calculate  $G_z$  numerically. Then we draw the contour plot of  $G_z$  to obtain the reconstruction of  $\partial D$ . The choice of reconstruction of  $\partial D$  could be the first reasonable closed iso-curve of  $G_z$ . In Figures 6 and 7, we show the contour plot of  $G_z$  for the sound soft obstacle and the inhomogeneous medium, respectively. For both cases, the reconstructions provide good approximations of the targets' boundaries.

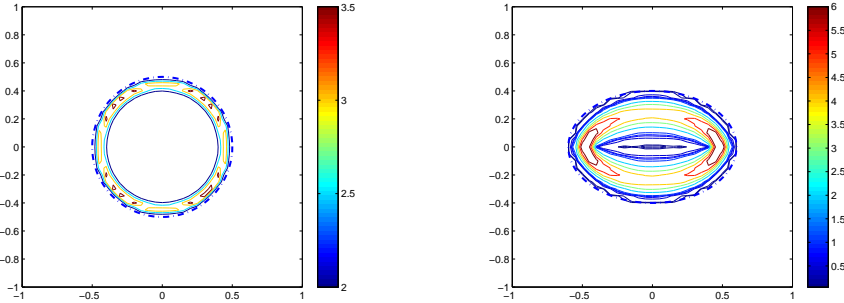


Figure 6: Reconstruction (contour plot of  $G_z$ ) of the sound soft obstacles using the gradient indicator. Left: The target is a disk with  $r = 1/2$ . Right: The target is an ellipse whose axes are 0.6 and 0.4.

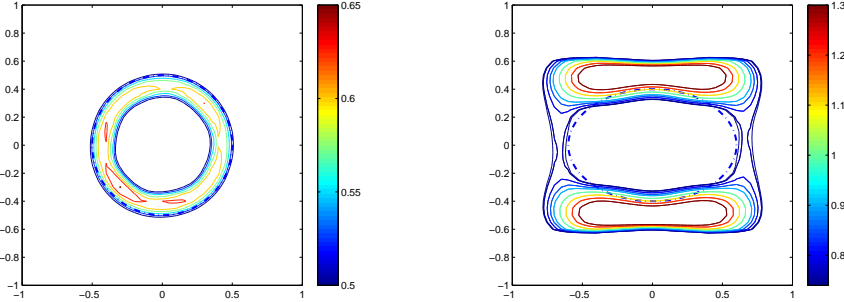


Figure 7: Reconstruction (contour plot of  $G_z$ ) of inhomogeneous media by using the gradient indicator. Left: The target is a disk with  $r = 1/2$ . Right: The target is an ellipse whose axes are 0.6 and 0.4.

### 3.3 Estimation of the eigenvalues

After we obtain the reconstruction of the target, we can locate the eigenvalues by choosing a point  $z$  in  $D$  and plotting  $H_z(k_i)$ . We can choose a couple of points and plot the corresponding  $H_z(k_i)$ . For the sound soft obstacle, from the above reconstruction in Fig. 4 or Fig. 6, it is easy to see  $(0, 0)$ ,  $(0.2, 0.1)$  and  $(-0.2, 0.2)$  are inside the circular target. We plot  $H_z(k_i)$  corresponding to these three points in the left picture of Fig. 8. The presence of an eigenvalue can be seen clearly. The result is consistent with those in Section 2. We choose the same points for the ellipse and obtain similar results (see the right picture of Fig. 8).

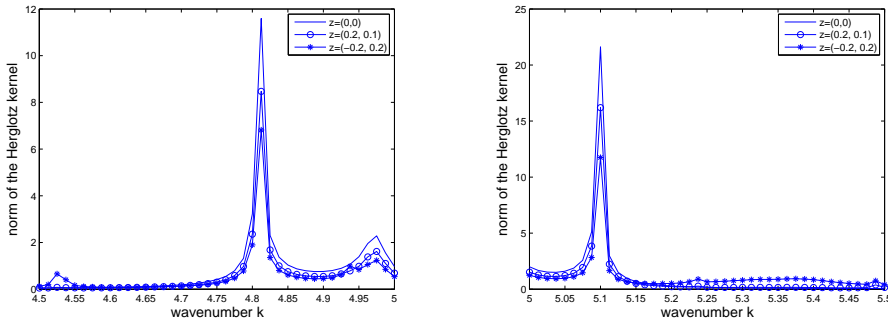


Figure 8: The plot of  $H_z(k_i)$  for different points  $z = (0, 0)$ ,  $z = (0.2, 0.1)$  and  $z = (-0.2, 0.2)$  inside the target for the sound soft obstacle. Left: The target is a disk with  $r = 1/2$ . Right: The target is an ellipse whose axis are 0.6 and 0.4.

For the inhomogeneous medium, we choose three points  $(0, 0)$ ,  $(0.2, 0.1)$  and  $(-0.2, 0.1)$  and show the result in Fig. 9. It can be seen that the estimation of the eigenvalues is rather stable with respect to the location of  $z$  inside the target for both scattering problems.

### 3.4 Distinguish between a sound soft obstacle and an inhomogeneous medium

Having reconstruction of  $D$  and estimation of eigenvalues, we can distinguish between a sound soft obstacle and an inhomogeneous medium. Since we obtain a rather accurate reconstruction of  $D$ , we can compute the Dirichlet eigenvalues. If these Dirichlet eigenvalues agree with the eigenvalues we obtain in the previous sub-section, the target is a sound soft obstacle. Otherwise, the target is a non-absorbing inhomogeneous medium. Note that the distribution of (real) transmission eigenvalues are more complicate than Dirichlet eigenvalues and it is not likely they coincide [13] (see Fig. 10).

## 4 Discussion and future work

In this paper, we propose an eigenvalue method using multiple frequency data (EM<sup>2</sup>F). The method can obtain accurate reconstruction of the target, esti-

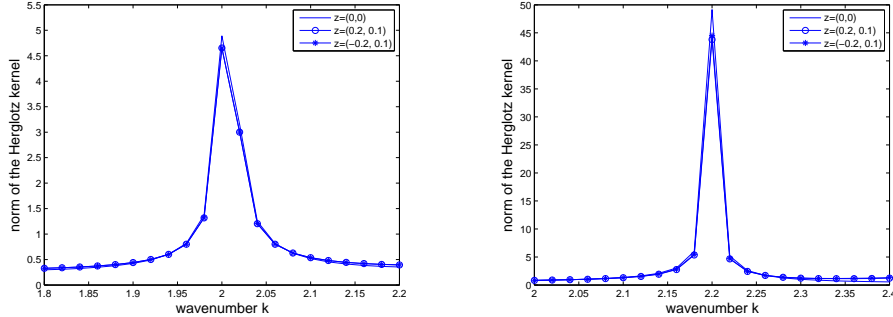


Figure 9: The plot of  $H_z(k_i)$  for different points  $z = (0, 0)$ ,  $z = (0.2, 0.1)$  and  $z = (-0.2, 0.1)$  inside the target for the inhomogeneous medium. Left: The target is a disk with  $r = 1/2$ . Right: The target is an ellipse whose axis are 0.6 and 0.4.

mate Dirichlet or transmission eigenvalues, and distinguish between a sound soft obstacle and a non-absorbing inhomogeneous medium. Comparing to the LSM using single frequency data, the method could provide better and more stable reconstruction for certain cases. For the LSM, the choice of iso-curve as the reconstructed boundary of the target is usually done by using the heuristic calibration approach which may not be reliable sometimes [8, 18]. The reconstruction also depends on the particular wave number which could be a restrictive condition when the size of the object is not known a priori. In addition, the standard LSM (at least theoretically) avoids eigenvalues unless special treatment is employed (see [27]). For the EM<sup>2</sup>F, the contrast of the eigenvalue indicators for  $z$  inside and outside  $D$  is large and the value changes rapidly across the boundary for the numerical examples we consider. Thus the cut-off value can be chosen easily. For the gradient indicator, it is even simple since one can choose the iso-curve whenever a close curve is formed.

The goal of this paper is to introduce the idea of the EM<sup>2</sup>F and show its potential use in inverse scattering with simple examples. Obviously a paper like this raises more questions than it answers. Among them, how to theoretically justify the behavior of the solutions of the ill-posed integral equations for  $z \in \partial D$  and outside  $D$  when  $k$  is an eigenvalue is highly desirable. Furthermore, the choice of the interval  $F_k$  and the corresponding partition  $F_k^i$  should also be elaborated. We refer the readers to [16] which contains interesting examples related to the problems we discussed above.

In this paper, we only test two scattering problems, namely, the sound soft object and the non-absorbing medium. Other types of scattering objects should be investigated. The EM<sup>2</sup>F can be extended to the case of the far field data in the same way. In addition, one expects that other qualitative methods such as the reciprocity gap method [9, 15, 23] and the factorization method [19] can also be applied and should obtain similar results.

Note that the method do need a lot of data and computation. It becomes more expensive if one considers three dimensional problems. However, the EM<sup>2</sup>F is essentially parallelizable. This is due to the fact that processing of

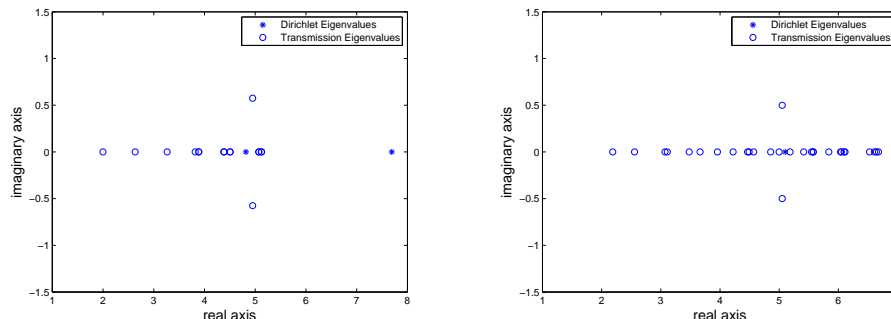


Figure 10: Distribution of Dirichlet eigenvalues and transmission eigenvalues in the complex plane. Transmission eigenvalues are corresponding the constant index of refraction  $n = 16$ . Note that there exist complex transmission eigenvalues. Left: The target is a disk with  $r = 1/2$ . Right: The target is an ellipse whose axis are 0.6 and 0.4.

a point  $z$  in the sampling domain is totally independent on other points. In fact, even for a fixed point  $z$ , the processing of the ill-posed integral equations corresponding to different wave number  $k$  is independent. It would be interesting to parallelize the method for three dimensional problems.

## Acknowledgements

The research was supported in part by NSF under grant DMS-1016092.

## References

- [1] F. Cakoni and D. Colton, *Qualitative Methods in Inverse Scattering Theory*, Springer, Series on Interaction of Mathematics and Mechanics, 2006.
- [2] F. Cakoni, D. Colton and H. Haddar, *On the determination of Dirichlet and transmission eigenvalues from far field data*, *C. R. Acad. Sci. Paris, Ser. I* 348 (2010), 379–383.
- [3] F. Cakoni, D. Colton, P. Monk and J. Sun, *The inverse electromagnetic scattering problem for anisotropic media*, *Inverse Problems* 26 (2010) 074004.
- [4] F. Cakoni, D. Colton and P. Monk, *On the use of transmission eigenvalues to estimate the index of refraction from far field data*, *Inverse Problems* 23 (2007), 507–522.
- [5] F. Cakoni, D. Colton and J. Sun, *Estimation of transmission and Dirichlet eigenvalues by near field linear sampling method*, *Proceedings of the 10th International Conference on the Mathematical and Numerical Aspects of Waves*, Vancouver, Canada, July 25-29, 2011, 431–434. accepted.

- [6] F. Cakoni, D. Gintides and H. Haddar, *The existence of an infinite discrete set of transmission eigenvalues*, SIAM J. Math. Analysis. Vol. 42 (2010), No 1, 237–255.
- [7] Q. Chen, H. Haddar, A. Lechtleiter, and P. Monk, *A sampling method for inverse scattering in the time domain*, Inverse Problems, 26(2010) 085001.
- [8] D. Colton, J. Coyle, and P. Monk, *Recent developments in inverse acoustic scattering theory*, SIAM Rev., 42 (2000), pp. 369–414.
- [9] D. Colton and H. Haddar, *An application of the reciprocity gap functional to inverse scattering theory*, Inverse Problems 21 (2005), 383–398.
- [10] D. Colton and A. Kirsch, *A simple method for solving inverse scattering problems in the resonance region*, Inverse Problems 12 (1996), 383-393.
- [11] D. Colton and R. Kress, *Inverse acoustic and electromagnetic scattering theory*, 2nd Edition, Springer-Verlag (1998).
- [12] D. Colton and P. Monk, *A novel method for solving the inverse scattering problem for time-harmonic acoustic waves in the resonance region*. SIAM J. Appl. Math. 45 (1985), no. 6, 1039-1053.
- [13] D. Colton, P. Monk and J. Sun, *Analytical and computational methods for transmission eigenvalues*, Inverse Problems 26 (2010) 045011.
- [14] D. Colton, L. Päiväranta and J. Sylvester, *The interior transmission problem*, Inverse Problem and Imaging, Vol. 1 (2007), No. 1, 13–28.
- [15] M. Di Cristo and J. Sun, *An inverse scattering problem for a partially coated buried obstacle*, Inverse Problems 22 (2006), 2331–2350.
- [16] B. Guzina, F. Cakoni and C. Bellis, *On multi-frequency obstacle reconstruction via linear sampling method*, Inverse Problems 26 (2010), 125005.
- [17] G. Hsiao, F. Liu, J. Sun, and L. Xu, *A coupled BEM and FEM for the interior transmission problem in acoustics*, Journal of Computational and Applied Mathematics, Vol. 235 (2011), Iss. 17, 5213–5221.
- [18] J. Li, H. Liu and J. Zou, *Strengthened linear sampling method with a reference ball*, SIAM J. Sci. Comput. 31 (2009/10), no. 6, 4013–4040.
- [19] A. Kirsch and N. Grinberg, *The factorization method for inverse problems*, Oxford University Press, 2008.
- [20] A. Kirsch, *On the existence of transmission eigenvalues*, Inverse Problems and Imaging, Vol. 3 (2009), No. 2, 155–172.
- [21] D.R. Luke and R. Potthast, *The point source method for inverse scattering in the time domain*, Math. Meth. Appl. Sci., 29 (2006), 1501-1521.
- [22] L. Päiväranta and J. Sylvester, *Transmission eigenvalues*, SIAM J. Math. Anal., Vol. 40 (2008), No. 2, 738–753.
- [23] P. Monk and J. Sun, *Inverse scattering using finite elements and gap reciprocity*, Inverse Problems and Imaging, Vol. 1, No. 4, 2007, 643–660.

- [24] B.P. Rynne and B.D. Sleeman, *The interior transmission problem and inverse scattering from inhomogeneous media*, SIAM J. Math. Anal., Vol. 22 (1991), No. 6, 1755–1762.
- [25] J. Sun, Estimation of transmission eigenvalues and the index of refraction from Cauchy data, *Inverse Problems* 27 (2011) 015009.
- [26] J. Sun, *Iterative methods for transmission eigenvalues*, SIAM Journal on Numerical Analysis, accepted.
- [27] W. Muniz, *A modified linear sampling method valid for all frequencies and an application to the inverse Inhomogeneous medium Problem*, Proc. Appl. Math. Mech. 5 (2005),689-690.